ISSN 1063-7729, Astronomy Reports, 2024, Vol. 68, No. 3, pp. 257–267. © Pleiades Publishing, Ltd., 2024.

Probing the Ionosphere with Pulses from the Pulsar B2016+28 at a Frequency of 324 MHz

M. S. Burgin[a],* and M. V. Popov[a],**

[a]*Astrospace Center of Lebedev Physical Institute of the Russian Academy of Sciences, Moscow, Russia*

**e-mail: mburgin@asc.rssi.ru*

***e-mail: popov069@asc.rssi.ru*

Received November 22, 2023; revised January 4, 2024; accepted January 29, 2024

Abstract—Using ground-space VLBI data from the RadioAstron project archive, the phase distortions of the cross-spectrum caused by the ionosphere have been calculated and their influence on the results of determination of the visibility function has been studied. The Arecibo Observatory's 300-m antenna served as the ground station for the interferometer. The separation of ionospheric phase distortions from the influence of the interstellar and interplanetary medium and instrumental errors is based on different frequency dependencies of these effects. The amplitude of ionospheric phase variation caused by electron density fluctuations in the ionosphere above the Arecibo radio telescope is several radians per observation session of about one hour. The structure function of phase variations indicates a continuous spectrum of electron density fluctuations at typical times of $\gtrsim$2–5 min with no pronounced signs of quasi-periodic processes. Ionospheric phase fluctuations during pulsar observations increase the width of the maximum of the amplitude of the visibility function as a function of the residual fringe rate by 5–10 mHz with a decrease in the value at the maximum of ≈10%. When constructing images of radio galaxies and quasars from ground-based VLBI observations, these phase shifts can significantly distort the final results.

Keywords: pulsars, scintillation, interstellar medium, ionosphere

DOI: 10.1134/S1063772924700276

1. INTRODUCTION

The medium between ground-based radio telescopes and space radio sources has a strong influence on the propagation of radiation from these sources. The interaction of radio waves with inhomogeneities in the medium causes a number of effects that affect the results of interferometric measurements with very long baselines (VLBI): refraction, which leads to a change in the direction of propagation of radiation and, thereby, a shift in the apparent position of the source, and scattering, which causes blurring of the image of compact sources and fluctuations in their brightness—scintillations.

One of the main scientific tasks of the ground-space radio interferometer RadioAstron [1] were observations of pulsars. These observations were carried out primarily at 316 MHz. Since the emitting regions of pulsars are not resolved even on the maximum baseline projections of the RadioAstron, when interpreting the results of these observations, pulsars can be considered point sources, and the observed image structure is completely determined by the influence of the medium. Moreover, during observations at frequencies below 1 GHz, the main distortions arise when radiation passes through ionized components of the medium: interstellar plasma, solar wind plasma and the ionosphere.

Description of the main effects caused by the scattering of pulsar radiation on inhomogeneities of the interstellar plasma (time and frequency modulation of the flux density, broadening of pulses, etc.), can be found in Rickett's reviews [2, 3]. Basic parameters of interstellar scintillation—decorrelation band $\Delta f_{\rm dif}$ and characteristic scintillation time $\Delta t_{\rm dif}$ — are determined by the characteristics of the interstellar medium along the line of sight, and vary widely for different objects and show noticeable variability for a number of pulsars.

The main effect caused by the influence of solar wind plasma inhomogeneities on the propagation of radiation from compact radio sources is interplanetary scintillation, i.e., flux fluctuations caused by scattering. A description of the results of observations of interplanetary scintillation and conclusions drawn on their basis about the parameters of electron density fluctuations in the solar wind can be found in the works [4, 5].

The results of VLBI observations at low frequencies are significantly influenced by phase distortions that occur when radio waves pass through the ionosphere.

The study of these distortions is necessary for the correct interpretation of observational data on astronomical objects, and also allows us to obtain information about the processes occurring in the ionosphere above the telescopes participating in the observations.

Ionospheric effects affecting the propagation of radio waves have been studied in many publications using various methods. A review of works on this topic can be found, for example, in [6]. The application of VLBI to the problem under consideration is described by Zhi-Han and Yong [7], Hobiger, Kondo and Schuch [8] and Heinkelmann, Hobiger and Schmidt [9]. In the work of Zhuravlev et al. [10] one can find a more modern review of publications concerning the influence of the ionosphere on the propagation of radio signals.

In the context of ground-space VLBI observations, the influence of ionospheric and interplanetary plasma was first discussed by Denison and Booth [11] back in 1987 when discussing the international program for creating a ground-space radio interferometer. They considered the feasibility of installing a 327 MHz receiver on board the space telescope in connection with distortions caused by irregularities in the ionosphere and in the solar wind.

Three types of ionospheric variations were identified: slow diurnal variations, moving ionospheric disturbances, and fast random electron density fluctuations, and the influence exerted by the frequency and time dependence of phase distortions on the amplitude of the visibility function was studied. Calculations have shown that since in the considered range ionospheric distortions weakly depend on frequency, then when observing at the zenith, the frequency decorrelation caused by them can be neglected in the frequency band up to 18 MHz in the daytime and in the band up to 58 MHz at night. According to estimates given in [11]. Slow daily variations in electron density in the ionosphere blur the visibility function along the fringe rate within 20 mHz, and the contribution of random fluctuations is negligible ($\ll$1 rad). According to the authors, only moving ionospheric disturbances that arise during certain geophysical phenomena associated with large energy release (magnetic storms, lightning storms, etc.) could have a noticeable impact on the amplitude of the visibility function. The characteristic time of these disturbances ranges from several minutes to tens of minutes.

Also in [11], the influence of solar wind inhomogeneities responsible for interplanetary scintillations on the results of VLBI observations was studied. An estimate of phase distortions due to fluctuations in the density of interplanetary plasma for the configuration of the ground-space interferometer used in this work gave the value $\lesssim$0.3 rad when observing in the antisolar hemisphere.

As part of the RadioAstron project [1], numerous VLBI observations of pulsars were carried out with ground-space bases, and their results confirmed the predictions of Denison and Booth, Shishov, et al. [12] during observations of the pulsar B1919+21 at the Green Bank-Westerbork base, noticeable periodic variations were discovered in the phase of the cross-spectrum harmonics with a characteristic period ≈70 s. According to their estimates, these variations do not have a significant impact on the results of measuring the visibility function at ground-space bases.

Zhuravlev et al. [10] purposefully assessed the influence of the ionosphere on the results of VLBI observations of the pulsar B0950+08 with the ground-space interferometer RadioAstron. The authors found significant synchronous half-hour variations in the total electron content (TEC) in the ionosphere at the intercontinental distance between the Arecibo and Westerbork stations. It turned out that the TEC values in the discovered structures are approximately twice as high as the TEC values outside these structures. According to preliminary analysis, the discovered structures were observed during a geomagnetic storm.

Popov et al. [13] discovered noticeable quasi-periodic variations in the scintillation phase in the cross-spectrum of the pulsar B0329+54 at the base between the space radio telescope and the 110-m radio telescope of the Green Bank Observatory with characteristic time with scales of 12 and 10 min and amplitudes up to 6.9 rad. Observations were carried out in the frequency range 316–332 MHz in four sessions on November 26–29, 2012 with gradually increasing baseline projections of 60, 90, 180, and 240 thousand kilometers. In two out of four sessions, quasiperiodic phase variations were detected. The authors attribute these changes to the influence of moving medium-scale ionospheric disturbances. The measured amplitude corresponds to variations in the vertical TEC in the ionosphere around 0.1×10^{16} m^{-2}. Such changes would significantly limit the coherent integration time in VLBI studies of compact radio sources.

In this work, we continue to analyze the influence of ionospheric disturbances on the results of ground-space radio interferometry, using data obtained from observations of the pulsar B2016+28 in the RadioAstron project.

2. THEORETICAL INTRODUCTION, OBSERVATIONS AND PRELIMINARY REDUCTION OF MEASUREMENT RESULTS

The results of interferometric observations of interstellar scattering are usually presented in the form of a dynamic cross-spectrum

$$Z = \left\langle \tilde{E}_A(f,t)\tilde{E}_B^*(f,t)\right\rangle, \quad (1)$$

where $\tilde{E}_A(f,t)$ and $\tilde{E}_B(f,t)$—Fourier components of electric fields of signals received at stations A and B, superscript * means complex conjugation, and $\langle\ldots\rangle$ — averaging over time. Ionospheric effects do not affect the amplitude of the signal field, so only the cross-spectrum phase can serve as a source of information about them.

From (1), it is clear that the phase Z equal to the phase difference of the signals received at the stations. If all observations are carried out from the Earth's surface, then it is possible to separate the contributions to variations in the cross-spectrum phase associated with different telescopes only with the use of additional information. Such a separation becomes trivial in the case when one of the interferometer arms is placed in space, since in this case, the phase distortions depend only on the state of the ionosphere above the ground station.

This work uses the results of observations conducted on May 22, 2015 in the band 316–332 MHz. A full description of the experiment is given in the work [14], in that paper, by analyzing the dynamic spectrum obtained with a ground-based telescope, the values of the decorrelation band were calculated $\Delta f_{\mathrm{dif}} = 43 \pm 2$ kHz and flicker time $\Delta t_{\mathrm{dif}} = 2125$ s. Ionospheric phase variations were estimated by processing measurements obtained from the Arecibo SRT in left-hand circular polarization.

2.1. Correlation Processing and Preliminary Signal Averaging

During correlation processing, which was carried out using the method described in [15] correlator of the ASC of Lebedev Physical Institute, the band was divided into 4096 channels wide $\Delta^{\mathrm{c}} f \approx 3.91$ kHz, and the time interval for issuing correlator data (interrogation time) was equal to the pulsar period and amounted to $\Delta^{\mathrm{c}} t \approx 0.56$ s with a total observation duration of 55 min. The accumulation of the correlation result (integration time) was carried out in two windows during the pulsar period: in the "signal" window, including the main pulse, and in the "noise" window outside the pulse, which was used to estimate the contribution of system noise to the observed signal; The duration of each window was 28 ms. The auto-spectrum obtained in the noise window at the Arecibo telescope was used to clear the processed data from noise. Frequency channels numbered 992–1048 and 1472–1548, in which Arecibo recorded an intense, highly variable signal outside the pulse, were completely excluded from processing.

Next, to increase the signal-to-noise ratio, the dynamic cross-spectra obtained at the correlator output were averaged over time with the duration of the averaging interval $\Delta^{\mathrm{a}} t = 16\Delta^{\mathrm{c}} t \approx 8.96$ s and frequency with averaging band $\Delta^{\mathrm{a}} f = 8\Delta^{\mathrm{c}} f \approx 31.3$ kHz. Below, for brevity, the term "pixel" will be used for the region of averaging of the dynamic cross spectrum. The averaged cross spectrum in the signal window is a function $Z^{(a)}(j,k)$, where $j = 1$–512 and $k = 1$–325—numbers of averaging intervals by frequency and time, respectively. Calculation results $Z^{(a)}$ are illustrated in the top graph of Fig. 1.

In the figure, the color of each pixel is determined by the phase of the cross spectrum $\arg(Z^{(a)})$, and brightness by its module $\left|Z^{(a)}\right|$. The horizontal black bars correspond to interscan gaps, and the vertical ones correspond to frequencies that were excluded from processing due to interference at the ground station. The pixel sizes are chosen so that the inequalities are satisfied $\Delta^{\mathrm{a}} f < \Delta f_{\mathrm{dif}}$ and $\Delta^{\mathrm{a}} t < \Delta t_{\mathrm{dif}}$ and averaging do not noticeably distort the picture of the variability of the dynamic cross-spectrum caused by interstellar scintillations.

To estimate the errors introduced by system noise, the pre-averaging algorithm described above was applied to the dynamic cross-spectrum obtained by correlating the signal outside the pulsar pulse. Statistical analysis of the noise cross-spectrum of the system obtained in this way showed that its real and imaginary parts, as would be expected during normal operation of the equipment, are independent normally distributed random variables. The standard deviation of these random variables, denoted below as $\sigma(t, f)$, does not depend on time t, but changes noticeably with frequency f (see Fig. 2).

2.2. Phase Variations in Scintles

The general picture of the brightness distribution shown in Fig. 1 dynamic cross spectrum is similar to the brightness distribution in the dynamic auto spectrum obtained in [14] according to measurements in Arecibo: in both spectra, a number of scintles—regions of increased brightness—are observed with a lifetime comparable to the duration of the session, and practically not drifting in frequency.

Scintles observed in dynamic spectra are one of the manifestations of the microstructure of scattering disks. Because observations from large ground-space bases can resolve speckles (microstructure features) in the scattering disk, the contributions of individual speckles to the observed cross-spectrum may have different phases. Accordingly, the phase of the visibility function may be different for scintles formed by the radiation of different speckles.

That phase of $Z^{(a)}$ really varies greatly from scintle to scintle can be easily seen in Fig. 1. A more careful analysis also shows that within almost all scintillas the phase is weakly dependent on frequency. The exceptions are several of the most extended scintillas in frequency. Apparently, these extended scintles are a

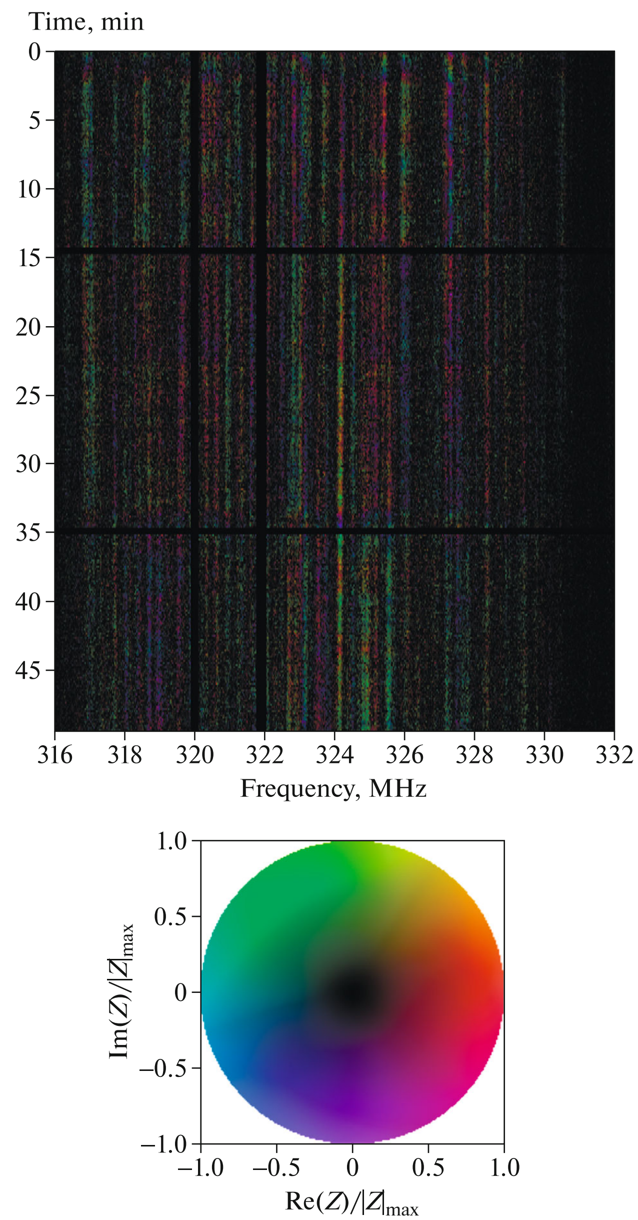

Fig. 1. The top graph is the observed dynamic cross-spectrum based on RA-AR. For each cross-spectrum point, the averaged complex value $Z^{(a)}(f, t)$ is mapped to a point on the unit color wheel as illustrated in the bottom graph, $\left|Z^{(a)}\right|_{\max}$—maximum value of the cross-spectrum modulus.

superposition of two or more scintillas, which have different phases, since they are formed by the radiation of different speckles.

Further analysis used the measurement results in $M = 20$ selected scintillas, which were approximated by rectangles $j_1(s) \le j \le j_u(s)$, $k_1(s) \le k \le k_u(s)$ in the averaged cross spectrum. Here and below the index $s = 1,\ldots,M$ identifies scincil.

For each selected scintle, the cross-spectra averaged over cross-section $t = \text{const}$ were calculated

$$Z_s(k(t)) = \frac{1}{L_s}\sum_{j=j_1(s)}^{j_u(s)} Z^{(a)}(j,k), \qquad (2)$$

where $L_s = j_u(s) - j_1(s) + 1$—extent of scintle s in frequency in pixels, $k(t)$—number of the time averaging interval corresponding to the time t. Since only scintles were identified with a small extent in frequency and a cross-spectrum phase that varied slightly between the low- and high-frequency boundaries of the scintle, then within the scintle s the change in the phase of the cross spectrum is completely described by the dependence $Z_s(k)$, and the system noise $\sigma(f)$ can be considered constant and approximated by $\sigma(f) = \sigma_s$.

3. CALCULATION OF THE IONOSPHERIC CONTRIBUTION TO THE CROSS-SPECTRUM PHASE

Measured cross-spectrum value in scintle s can be represented as $Z_s(t) = Z(f_s,t) + z_s(t)$, where Z—cross-spectrum of the signal received by the interferometer antennas, z_s—measurement errors, f_s—average frequency of the scintillum. For further analysis, let us present the cross-spectrum in exponential form $Z(t) = |Z(t)|\exp(i\phi(t))$ and similarly for $Z^{(a)}(t)$ and $Z_s(t)$.

Variations in Z are caused by the pulsar's own variability, interstellar and interplanetary scintillations, and ionospheric disturbances, and changes in the ionospheric electron content do not affect $|Z(t)|$, and the intrinsic variability of the pulsar do not affect $\phi(t)$. When observing near the zenith, as was the observations in our observations at Arecibo, the ionospheric phase shift is given by the relation [16, 17]

$$\phi_{\text{atm}} = -8.45\frac{C_e}{10^{16}\ \text{m}^{-2}}\frac{1\ \text{GHz}}{f}\sec\zeta, \qquad (3)$$

where ζ—zenith angle of the pulsar, C_e—TEC in the ionosphere,

$$C_e = \int_0^\infty n_e(h)dh, \qquad (4)$$

where $n_e(h)$ is the dependence of electron density in the ionosphere on altitude.

When observations are carried out in a narrow frequency range, absolute measurements of the ionospheric phase shift are fundamentally impossible, since the values $\phi^{(a)}(t)$, which are the only source of information about variability C_e, are determined ambiguously, up to a term $2n\pi$, where n—unknown

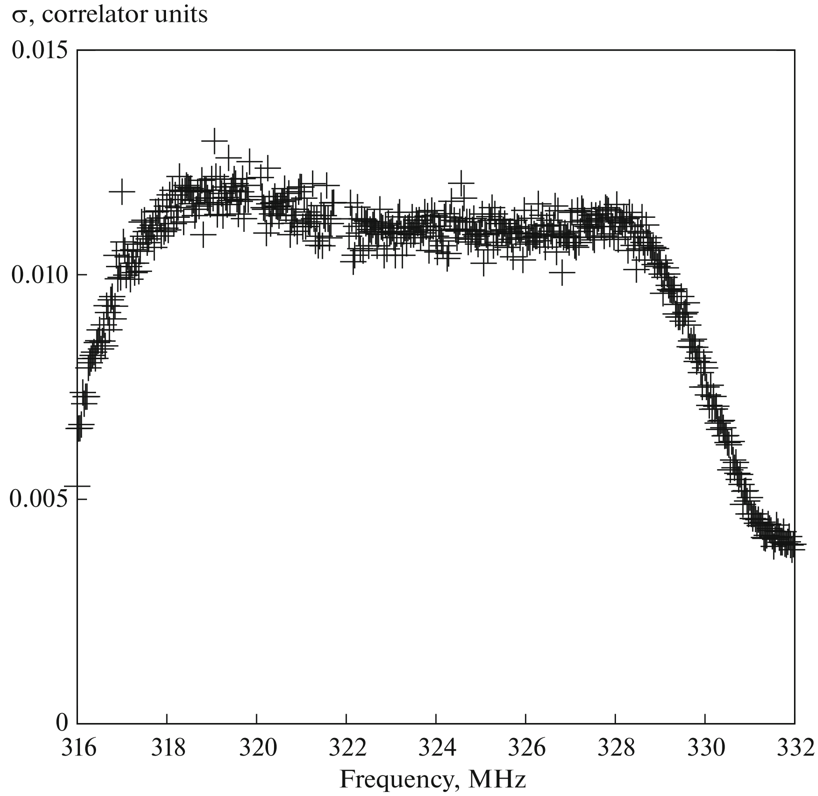

Fig. 2. System noise dependence σ from frequency.

integer. This is exactly the situation that occurs in the case under consideration, because $B/f_0 < 0.05$, where $B = 16$ MHz—bandwidth, $f_0 = 324$ MHz—center frequency.

If, however, we consider not the phase itself as the measured quantity $\phi(t)$, but its derivative $d\phi(t)/dt$, approximated by the divided difference between two successive measurements, then if the interval between measurements is sufficiently small, this ambiguity does not affect the result. Since the values $Z^{(a)}$ were measured with period ≈8.96 s, significantly less than the characteristic time of change $\phi(t)$, the $2\pi n$-ambiguity is easily resolved in measuring $d\phi(t)/dt$.

Since the purpose of the calculations described below will be to estimate $d\phi(t)/dt$, then the main quantities appearing in further analysis will be

$$\Delta\phi(t',t'') = \phi(t'') - \phi(t') \tag{5}$$

—change in the phase of the true cross spectrum between two moments t' and t'', and the corresponding quantities directly obtained from measurements

$$\Delta\phi_s(t',t'') = \phi_s(t'') - \phi_s(t'). \tag{6}$$

Next, we will mainly consider the phase difference for two consecutive pixels ($t'' - t' = 8.96$). Typically, in this case, for the sake of brevity, the arguments t' and t'' will not be stated explicitly.

3.1. Separation of the Contributions of the Ionosphere and the Interstellar Medium to Phase Variations

Since the phase of the cross spectrum changes not only due to variations C_e, but also due to interstellar and interplanetary scattering, then for further analysis we express the phase change at the scintillium frequency s as

$$\Delta\phi(f_s) = \theta(f_s) + \eta(f_s), \tag{7}$$

where θ is the sum of the contributions of the ionosphere and interplanetary plasma, and η—contribution of the interstellar medium.

The nature of the physical processes that determine the values $\theta(f_s)$ and $\eta(f_s)$, is the same—the interaction of pulsar radiation with fluctuations in the refractive index caused by variations in electron density. However, quantitatively, the solutions to the radiative transfer equation describing these two terms correspond to two opposite asymptotic regimes. Namely, in the frequency range we use, interstellar scintillations of the pulsar B2016+28 are described by the strong scattering approximation, while interplanetary and ionospheric effects are described by the weak scattering approximation. For the two indicated scattering modes, the frequency dependence of the properties of scattered radiation is very different (see, for example, [3]), which allows us to separate the contribution of the two terms on the right side (7).

Strong scattering in interstellar plasma causes deep—with an amplitude of almost 100%—modulation of the signal as a function of time and frequency, which leads to the formation of scintles in the dynamic auto- and cross-spectra of pulsars (see Fig. 1). Individual scintles are formed by radiation coming from geometrically separated and physically independent regions of the interstellar medium. Therefore, the values $\eta(f_s)$ for different index values s are independent random variables and averaging over a large number of scintillas observed in the dynamic cross-spectrum of the pulsar B2016+28 makes it possible to reduce the contribution made by interstellar scattering to the measurements $\Delta\phi(f_s)$.

With weak scattering, the characteristics of the scattered radiation change little within the relatively narrow frequency range used in the observations described here. Therefore, averaging over individual scintles has virtually no effect on the contribution of the term $\theta(f_s)$ in (7).

Separate in a similar way the influence of scattering on solar wind inhomogeneities from the ionospheric contribution to the value $\theta(f_s)$ impossible because the frequency dependence is weak for both of these effects. The following considerations show, however, that in the problem considered in this work, the influence of interplanetary plasma can apparently be completely neglected.

Firstly, since the solar wind density decreases approximately as $1/r^2$ with increasing distance from the Sun r, then all effects associated with interplanetary scattering quickly decrease with increasing angular distance of the observed source from the Sun and become extremely weak when observed in the antisolar hemisphere. According to technical restrictions on the orientation of the space radio telescope in the RadioAstron project, the angular distance between the line of sight and the Sun should be greater 90°; in our case this angle was ≈98°.

Secondly, ionospheric fluctuations and variability associated with solar wind inhomogeneity have significantly different temporal characteristics. This distinction was used, in particular, in the work [18] to separate ionospheric and interplanetary scintillations in observations with the LOFAR telescope. According to [19], correlation coefficient of interplanetary plasma density as a function of spatial coordinates r close to $\exp(-r^2/a^2)$, where $a \approx 250$ km in Earth orbit. This means that temporarily the structure function of fluctuations caused by interplanetary plasma in our data should quickly reach an asymptotic constant value with delays $\gtrsim 1$ s. Shown below (see Fig. 3), the results show a monotonic increase in the structural function up to delays ≈120 s, which indicates the dominant influence of the ionospheric component and the possibility of neglecting the influence of interplanetary scintillations in our consideration.

In the frequency range we use, near the zenith $\theta(f) \propto 1/f$, and due to the small relative width of the band, the difference between $\theta(f)$ and $\theta(f_0)$—values at the central frequency—does not exceed 2.5% over the entire frequency range. Therefore, to a first approximation, we can consider the ionospheric contribution to be the same for all scincils. Further, we will use this approximation and assume $\theta(f) = \theta$.

The algorithm used below for determining the ionospheric contribution to phase variations consists of two steps: (1) calculation of $\Delta\phi_s$ individually for each isolated scintle and (2) evaluation of θ by averaging the obtained values $\Delta\phi_s$ for every moment t, over all scintles for scintle which t enters the period of existence.

The rates of change in the phases of individual scintillas are easily found directly from observational data using the formulas (2) and (6), they were found to be confined mainly to the interval ±0.1 rad/s. This corresponds to the modulus of phase change over time $\Delta^a t$ less than 0.9 rad, so 2π-ambiguity does not affect further analysis.

To reduce errors caused by system noise and the influence of interstellar scattering, it is necessary to average the values $\Delta\phi_s$, calculated for individual scincilia. The averaging procedure, however, presents some difficulties and requires the use of a non-standard approach.

3.2. Estimate of θ *by Values* $\Delta\phi_s$

One of the primary sources of difficulties arising in estimating θ by averaging the measured values of $\Delta\phi_s$, is that the values $|Z|$ vary greatly both from scintle to scintle and depending on time. As a consequence, the influence of the noise component on $\Delta\phi_s$ varies over a wide range, which must be taken into account when averaging. If the errors of individual measurements differ, then the usual approach is to average with weights.

In a standard situation, it is optimal to assign weight for the every measurement of $\Delta\phi_s$ in individual scintilla $v_s = 1/(\mathrm{D}(\Delta\phi_s))$. Here and further $\mathrm{D}\xi$ denotes the variance of the random variable ξ.

However, in our case this approach is not applicable. The matter is that standard statistical methods are focused on the analysis of random variables and processes in Euclidean space. In our case, the phase value is determined only by absolute value 2π, then the range of values of the random process describing its

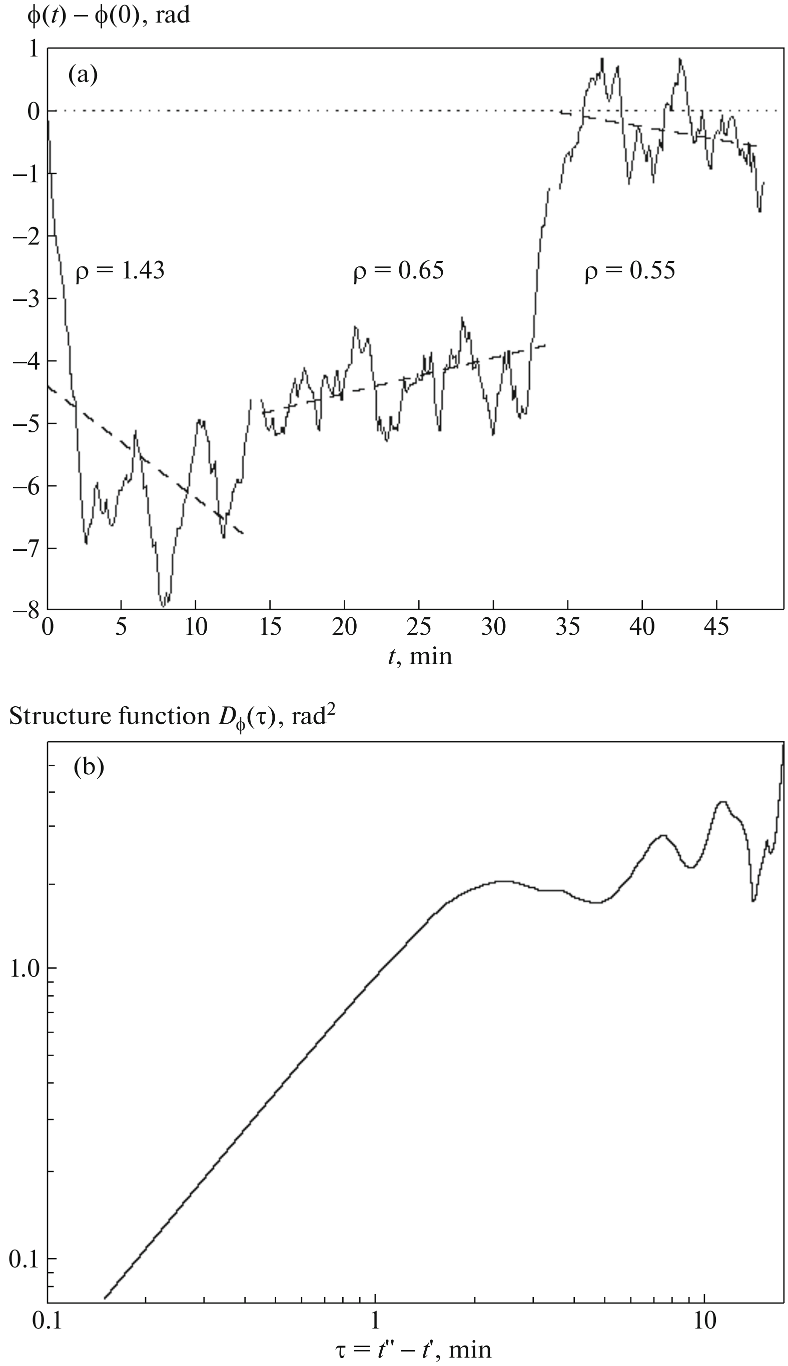

Fig. 3. (a) Dependence of the atmospheric contribution to the cross-spectrum phase variation ϕ_{atm} on time (solid line), its approximation by linear functions of time on each scan (dashed lines) and values ρ—root-mean-square deviations of the linear approximation from observations. (b) Structure function $D_\phi(\tau)$.

variability is a circle. As a result, statistical analysis of phase variations requires the use of specialized methods. Below we consider one of the possible approaches to solving this problem.

First of all, for a fixed point in time, we consider the effect of system noise on the accuracy of approximation of $\phi(f_s)$—phases of the true cross-spectrum in scintle s—by $\phi_s = \arg(Z_s)$, where Z_s defined in (6).

If the condition $|Z| \gg \sigma_s$ is met, i.e., when the signal in the pulse is larger compared to the noise level, then $Z \approx Z_s$ and the phase determination error is small. In this case, the fact that the range of values of the random variable $\phi(f_s) - \phi_s$ is a circle, and not a set of real numbers, can be neglected, and the standard approach applies. The variance of the phase determination error introduced by noise in this limit is given by the expression

$$D\phi_s \approx \sigma_s^2/(L_s|Z_s|^2) \ll 1, \quad (8)$$

and into expressions for various weighted averages Z_s comes with weight

$$w_s = L_s|Z_s|^2/\sigma_s^2. \quad (9)$$

If condition (8) is satisfied for all scintles taken into account when calculating the ionospheric phase shift, then the standard averaging procedure with weights is applicable. Namely, one can put

$$\theta = \frac{1}{u}\sum_s v_s \Delta\phi_s, \quad (10a)$$

where

$$\frac{1}{v_s(t',t'')} = \frac{1}{w_s(t')} + \frac{1}{w_s(t'')} \quad (10b)$$

and

$$u = \sum_s v_s. \quad (10c)$$

If scintles are involved in the averaging, for which the condition (8) is not satisfied, then standard methods for estimating the parameters of random distributions are not applicable. This manifests itself, in particular, in the fact that in the limiting case when $Z \to 0$ and therefore $Z_s \approx z_s$, weights calculated according to (9), do not decrease. As a consequence, averaging involves measurements containing only noise, which reduces the accuracy of the results.

To minimize the influence of measurements with low signal-to-noise ratio, the algorithm for calculating the weights must be modified. When analyzing observations of the pulsar B0329+54 in [13], this problem was solved by selecting only the strongest pulses for processing. In our notation, the algorithm used in that work is equivalent to the fact that the weights are calculated using the formula $w_s = H(|Z_s| - |Z|_{\text{th}})$, where H—Heaviside function, $|Z|_{\text{th}}$—a certain threshold value that ensures the fulfillment of the condition (8).

In the observations processed in this work, the proportion of measurements for which the condition (8) performed, too small. Therefore, it is necessary to use many measurements with a low signal level, compensating for the low individual accuracy of each individual measurement by averaging over a large number of them. This problem is solved algorithmically using in (10) properly selected function $w_s(Z_s)$ instead of (9).

For selection $w_s(Z_s)$, the following considerations can be used. At $Z_s \to \infty$, as was mentioned above, for optimal function $w_s(Z_s)$, the equality (9) must be asymptotically satisfied. In the opposite case, the signal is small compared to the noise, i.e., when the condition is met

$$|Z| \ll \sigma \quad (11)$$

optimal is $w_s = 0$. Since the directly measurable quantity is $Z_s = Z + z_s$, then to establish that the condition (11) is fulfilled, it is possible only with varying degrees of probability by testing the hypothesis $Z = 0$ using some statistical criterion. At the same time, to suppress the contribution of highly noisy measurements with $|Z| \ll \sigma$ should be in function $w_s(Z_s)$ introduce a factor tending to zero for those measurements for which the criterion used accepts the hypothesis being tested at high levels of significance.

If the hypothesis $Z = 0$ is true, then $Z_s = z_s$, and the sum

$$X_s^2 = \frac{1}{\sigma_s^2}\sum_{j=1}^{L_s}\left|Z^{(a)}\right|^2 = \frac{1}{\sigma_s^2}\sum_{j=1}^{L_s}\left|z^{(a)}\right|^2 \quad (12)$$

is distributed as $\chi^2_{2L_s}$, and to test the hypothesis about the small signal-to-noise ratio we used the criterion χ^2. To calculate the weights of the phase values measured in individual scintles, the following expression was used:

$$w_s = 2(\max(0, P(X_s^2) - 1/2))L_s|Z_s|^2/\sigma_s^2, \quad (13)$$

where $P(X_s^2)$—the probability that a random variable with a distribution function $\chi^2_{2L_s}$ takes a value less than X_s^2. For weights defined by (13) and $X_s^2 \to \infty$ the equality (9) is asymptotically satisfied. Measurements Z_s with such small values X_s^2 that the hypothesis $Z = 0$ is accepted at significance level $\alpha = 0.5$, are considered not to carry useful information. For them $w_s = 0$, and thus they are excluded from consideration.

After the weights w_s of individual measurements ϕ_s were calculated according to (13), calculation $\theta(t)$ carried out in the same way as in the case of the applicability of the standard approach, using Eqs. (10).

3.3. Calculation of Structure Functions of a Phase and Its Derivative

Further study of statistical properties $\theta(t)$ was performed using a method close to that used in the work [13] and based on an estimate of time structure function of the derivative of the phase

$$D_\theta(\tau) = \left\langle \delta^2(t',t'') \right\rangle, \quad (14)$$

where $\delta(t',t'') = \theta(t'') - \theta(t')$, and $\langle \ldots \rangle$ denotes averaging over all pairs of measurements $\theta(t'')$, $\theta(t')$ with

$t'' - t' = \tau$. Unlike [13], averaging in (14) was carried out taking into account the errors in measurements of θ.

To construct an averaging algorithm with weights similar to the one described by Eqs. (10) and (13) in this case is impossible for two reasons. Firstly, due to the quadratic dependence of the structure function on individual values $\theta(t)$, it is impossible to use an analogy with the results for linear statistical models. Secondly, the observed differences $\delta(t', t'')$ at the same values $t'' - t' = \tau$, but with different values of t' are associated not only with measurement errors, but also with the real variability of the ionospheric contribution to the cross-spectrum phase, and there is no detailed statistical description of this variability.

Due to these difficulties in calculating $D_\theta(\tau)$ weights assigned when averaging in (14) individual values of $\delta^2(t', t'')$, were chosen in the simplest way, compatible with the qualitative dependence of the error of $\delta^2(t', t'')$ on errors of $\theta(t'')$ and $\theta(t')$. Namely, the value $\delta^2(t', t'')$ was assigned the weight $\min(u(t'), u(t''))$, where $u(t)$ defined in (10). The results of calculations of $D_\theta(\tau)$ using the algorithm described above, they showed that, in contrast to a similar structure function obtained in [13], there are no obvious signs of quasiperiodic phase oscillations.

To assess the influence of ionospheric effects on the visibility function, it is necessary to consider the behavior of the phase, and not its derivative. Therefore, at the next processing stage for each scan by numerically integrating the function $\theta(t) = \phi'_{\text{atm}}$ we calculated the temporal dependence of the atmospheric contribution to the phase variation, and the corresponding structure function D_ϕ. The calculation results are illustrated in Fig. 3. Since in the interscan intervals $13.9 < t < 15.5$ min and $33.0 < t < 34.5$ min measurements are missing, then unambiguous phase recovery over the entire interval is impossible. When plotting the dependence $\phi_{\text{atm}}(t)$, it was assumed that the phase was constant in interscan intervals. When calculating $D_\phi(t'' - t')$, we included in the averaging only those terms $(\phi_{\text{atm}}(t') - \phi_{\text{atm}}(t''))^2$, for which both moments t' and t'' belong to the same scan, so the ambiguity of the phase shift between scans does not affect the result.

4. THE DISCUSSION OF THE RESULTS

Our work analyzes observations of the pulsar B2016+28, carried out at the Arecibo radio telescope on May 22, 2015, in a joint experiment with the RadioAstron space telescope. Since the Arecibo radio telescope is a transit instrument, the zenith distance of the direction to the source did not exceed a value of 15°. Observations were made at night, at approximately 4 o'clock local time, i.e., at least 2 h before sunrise. Thus, with an undisturbed ionosphere, the manifestation of ionospheric effects in this case should have been minimal.

The structural phase function contains information about the statistical properties of the TEC in the ionosphere; however, it is easier to study the influence of ionospheric effects on the results of processing VLBI observations in terms of the function itself $\phi_{\text{atm}}(t)$. The stage of such processing, following the acquisition of the cross-spectrum, is usually the calculation of the dependence of the interferometric visibility function $V(f_{\text{res}}, \Delta t)$ from the residual fringe rate f_{res} and delays Δt. In our case, this calculation was carried out separately for each scan. In order to analyze the influence of ionospheric disturbances on the diagram f_{res}–Δt, the ionospheric phase distortion measurements measured in each scan were expressed as

$$\phi_{\text{atm}}(t) = \phi_{\text{lin}}(t) + (\phi_{\text{atm}}(t) - \phi_{\text{lin}}(t)), \qquad (15)$$

where $\phi_{\text{lin}}(t)$—the best (in the sense of least squares) approximation of the function $\phi_{\text{atm}}(t)$ by a linear function of time, and the standard deviation of the linear approximation from the observations was calculated $\rho = \sqrt{\left\langle (\phi_{\text{atm}}(t) - \phi_{\text{lin}}(t))^2 \right\rangle}$ (see Fig. 3).

Influence of terms $\phi_{\text{lin}}(t)$ and $\phi_{\text{atm}}(t) - \phi_{\text{lin}}(t)$ in 34 function $V(f_{\text{res}}, \Delta t)$ completely different. This function is usually calculated by applying double Fourier transform to the dynamic cross-spectrum (inverse frequency transform and forward time transform). Since in the approximation we use, the phase shift occurs synchronously throughout the entire reception band, the distortions corresponding to the linear approximation are equivalent to the shift of the $V(f_{\text{res}}, \Delta t)$ along the fringe rate axis without changing the shape and do not change the internal structure of the scattering spot, which is derived from the visibility function at subsequent stages of processing.

In contrast, the term describing the nonlinearity of the dependence of the ionospheric phase shift on time leads to a distortion of the form of the function $V(f_{\text{res}}, \Delta t)$, in particular, to the "spreading" of the maximum modulus of the visibility function. These distortions are more noticeable the higher the value ρ, and increase the error in determining the structure of the scattering spot. A simple way to compensate for ionospheric distortions described by the nonlinear term in (15), by applying one or another transformation of the visibility function, apparently does not exist. Such a correction can only be performed by compensating for the phase variations we have detected before performing the Fourier transform in time, which is an integral part of the calculation algorithm $V(f_{\text{res}}, \Delta t)$.

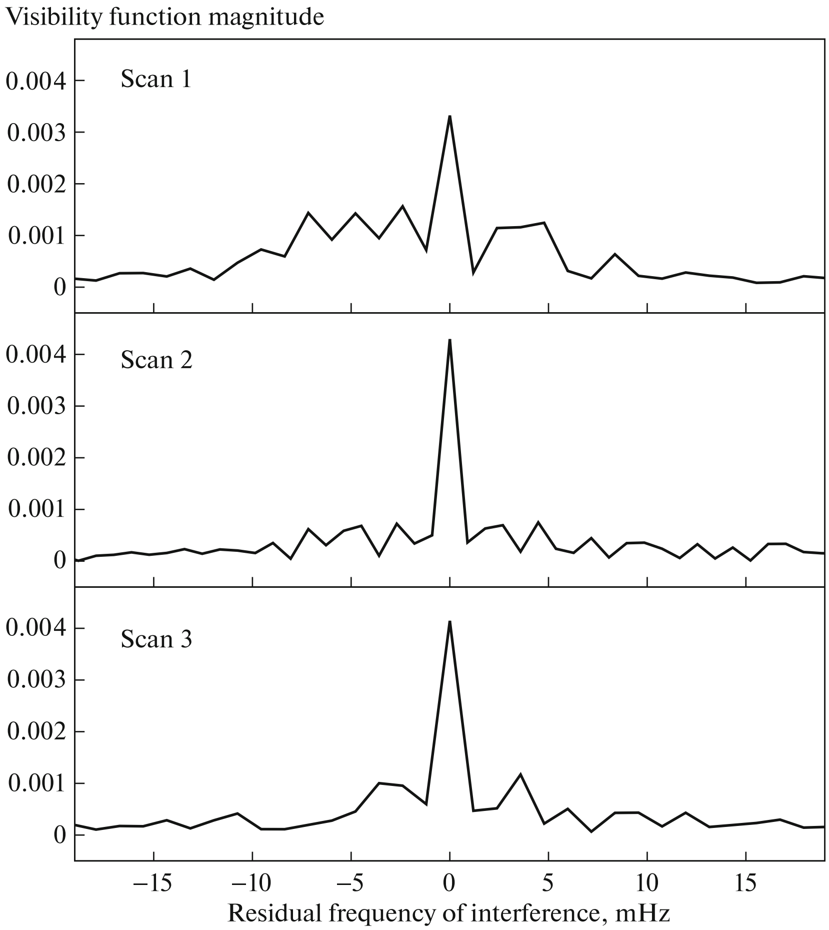

Fig. 4. Cross-section of the "residual fringe rate-delay" diagram by fringe rate at zero delay.

In Fig. 4, sections of the module of the visibility function are shown according to f_{res} at $\Delta t = 0$ for three observation scans. It can be seen that in the first scan, in which the value ρ more than twice the values for the other two scans, the peak of $|V(f_{\mathrm{res}}, 0)|$ is somewhat wider and lower. A comparison of the visibility function amplitudes for the three scans reveals differences within 10%.

Thus, we conclude that ionospheric effects in this experiment should not significantly affect the measurements of the amplitude of the visibility function depending on the projection of the base of the ground-space interferometer. Such measurements were presented in the work of Fadeev et al. [14]. They obtained the amplitude of the visibility function for this pulsar at a level of 0.26 with base projections from 89000 to 96000 km and determined the angular diameter of the scattering circle to be 2.1 mas.[1]

[1] mas (milliarcsecond)—angular millisecond of arc.

5. CONCLUSIONS

We used open archive data from the RadioAstron project, containing the results of correlation processing of VLBI observations of pulsars. We selected an hour-long observation session of the pulsar B2016+28, conducted on May 22, 2015 at ground-space baseline projections from 60000 to 90000 km. The 300-m radio telescope in Arecibo was used as a ground-based radio telescope. As was shown in the work [14], this pulsar has slow interstellar scintillations with a characteristic time of more than 30 min, which facilitates the separation of ionospheric and interstellar effects. Since the 10-m space radio telescope is located far beyond the Earth's ionosphere, the influence of the ionosphere affects the radio emission of the pulsar in its pure form, recorded by the ground-based telescope. Using an original technique for averaging complex cross-spectra, the temporal behavior of the phase of frequency scintles was obtained. The amplitude of these temporary phase changes do not exceed several radians during the entire interferometric session. The phase structure function shows that the characteristic time of phase fluctuations is 2–5 min.

An analysis of the influence of ionospheric disturbances on the results of pulsar observations shows that the distortions they cause in the modulus of the visibility function do not exceed 10%. However, the ionospheric distortions of the visibility function phase that we discovered may turn out to be critical for the task of constructing images of extended radio sources from observations on ground-based VLBI networks in the meter radio wave range. The phase closure method, for example, will not be applicable. We find an interesting option for VLBI observations in this range using a pulsar as a calibration source.

ACKNOWLEDGMENTS

The authors thank the reviewer for valuable comments and discussion.

FUNDING

The RadioAstron project was carried out by the Astrospace Center of the Lebedev Physical Institute Russian Academy of Sciences and the Lavochkin Research and Production Association under a contract with the State Corporation “ROSCOSMOS” together with many scientific and technical organizations in Russia and other countries.

CONFLICT OF INTEREST

The authors of this work declare that they have no conflicts of interest.

REFERENCES

1. N. Kardashev, V. Khartov, V. Abramov, V. Avdeev, et al., Astron. Rep. **57**, 154 (2007).
2. B. J. Rickett, Ann. Rev. Astron. Astropys. **15**, 479 (1977).
3. B. J. Rickett, Ann. Rev. Astron. Astropys. **28**, 561 (1990).
4. J. R. Jokipii, Ann. Rev. Astron. Astropys. **11**, 1 (1973).
5. S. K. Alurkar, *Solar and Interplanetary Disturbances, Astron. Astrophys. Series* (World Scientific, Singapore, 1997).
6. J. Aarons, Proc. IEEE **70**, 360 (1982).
7. Q. Zhi-Han and Z. Yong, in *Proceedings of the 156th Symposium IAU, Shanghai, China, September 15–19, 1992,* Ed. by I. I. Mueller and B. Kolaczek (Kluwer Academic, Dordrecht, 1993), IAU Symp. **156**, 207 (1993).
8. T. Hobiger, T. Kondo, and H. Schuh, Radio Sci. **41**, RS1006 (2006).
9. R. Heinkelmann, T. Hobiger, and M. Schmidt, in *Proceedings of the EGU General Assembly 2009, April 19–24, 2009, Vienna, Austria,* p. 5715. http://meetings.copernicus.org/egu2009
10. V. I. Zhuravlev, Y. I. Yermolaev, and A. S. Andrianov, Mon. Not. R. Astron. Soc. **491**, 5843 (2020).
11. B. Dennison and R. S. Booth, Mon. Not. R. Astron. Soc. **224**, 927 (1987).
12. V. I. Shishov, T. V. Smirnova, C. R. Gwinn, A. S. Andrianov, M. V. Popov, A. G. Rudnitskiy, and V. A. Soglasnov, Mon. Not. R. Astron. Soc. **468**, 3709 (2017).
13. M. V. Popov, N. Bartel, M. S. Burgin, T. V. Smirnova, and V. A. Soglasnov, Mon. Not. R. Astron. Soc. **506**, 4101 (2021).
14. E. N. Fadeev, A. S. Andrianov, M. S. Burgin, M. V. Popov, A. G. Rudnitskiy, V. I. Shishov, T. V. Smirnova, and V. A. Zuga, Mon. Not. R. Astron. Soc. **480**, 4199 (2018).
15. S. F. Likhachev, V. I. Kostenko, I. A. Girin, A. S. Andrianov, A. G. Rudnitskiy, and V. E. Zharov, J. Astron. Instrum. **6**, 1750004 (2017).
16. M. Mevius, S. van der Tol, V. N. Pandey, H. K. Vedantham, et al., Radio Sci. **51**, 927 (2016).
17. A. R. Thompson, J. M. Moran, and J. W. Swenson, Jr., *Interferometry and Synthesis in Radio Astronomy,* 3rd ed. (Springer, Cham, 2017).
18. R. A. Fallows, M. M. Bisi, B. Forte, T. Ulich, A. A. Konovalenko, G. Mann, and C. Vocks, Astrophys. J. Lett. **828**, L7 (2016).
19. A. C. S. Readhead, M. C. Kemp, and A. Hewish, Mon. Not. R. Astron. Soc. **185**, 207 (1978).